Scientia Iranica C (2019) 26(3), 1497–1504

Sharif University of Technology
Scientia Iranica
Transactions C: Chemistry and Chemical Engineering
http://scientiairanica.sharif.edu

Study of the effect of organic binders on 13X zeolite agglomeration and their CO_2 adsorption properties

M. Anbia* **and M. Aghaei**

Research Laboratory of Nanoporous Materials, Faculty of Chemistry, Iran University of Science and Technology, Narmak, Tehran 16846-13114.

Received 10 January 2017; received in revised form 4 February 2018; accepted 24 December 2018

KEYWORDS
Zeolite 13X;
Agglomeration;
Organic binder;
Mechanical strength;
CO_2 adsorption.

Abstract. The aim of the present research is to shape zeolite 13X and study the effect of singular and binary systems of binders. For this purpose, zeolite 13X was successfully synthesized under hydrothermal conditions. Different combinations of polyvinyl alcohol (PVA) and polyethylene glycol (PEG) were used for shaping. Physical properties of granules were measured by nitrogen adsorption-desorption, and results showed that increasing the binder content up to a certain amount enhanced the physical properties. However, the surface area decreased with a further increase in binder content. In addition, it was found that mechanical strength was decreased with increasing binder content after burnout.

1. Introduction

Zeolites are crystalline porous aluminosilicates with pores and channels. Zeolite structure is made of alumina and silica tetrahedra. These tetrahedra share their oxygen atoms and make a three-dimensional framework [1]. Each alumina tetrahedron in the framework has a negative charge, which is balanced by alkali and alkaline earth cations present in the voids of zeolite [2]. These cations are mobile due to their weak attraction and can be exchanged [3]. Silica-to-alumina ratio is a very effective parameter in properties of zeolite and can vary considerably from one to about 100 or more [4]. Zeolite 13X is a type of zeolite with a silica-to-alumina ratio of about 1-1.5 and Na^+ ions in its structure [5].

13X zeolite has the faujasite structure that consists of ten sodalite cages connected by hexagonal prisms. This structure forms an inner cavity of 7.4 Å that is called supercage [6] due to the high aluminum presence and the appropriate number of cations. Therefore, it has high ion exchange capacity and high affinity with polar molecules [7]. Zeolite X is of particular interest because of its remarkable properties and its use as an adsorbent [8-10], a catalyst [11,12], a molecular sieve [13], and an ion-exchanger [14,15]. Zeolite X has attracted widespread attention in many applications of modern science and technology, including removal of metal ions [16,17] and adsorption of gasses such as hydrogen [18,19], methane [20], oxygen [21], and carbon dioxide [22-26].

CO_2 is one of the natural gas components produced by combustion of fossil fuels and used as a by-product in industrial processes. This gas plays an important role in global warming; thus, capturing it by adsorption is one of the most important approaches in industrial applications [27]. There are several options for CO_2 adsorption [28-30]; however, zeolite 13X due to its high adsorption capacity, high adsorption rate, and high selectivity is one of the appropriate adsorbents [31].

Synthesized zeolites are in the powder form and

*. *Corresponding author. Tel.: +98 21 77240516; Fax: +98 21 77491204*
E-mail address: anbia@iust.ac.ir (M. Anbia)

doi: 10.24200/sci.2018.21198

must be agglomerated and make granules with high mechanical strength and high adsorption capacity used in industrial processes. Granulation is the process of joining particles together using a binder and forming granules. Binders are added to the mixture in low quantities that create bridges between particles and hold them together [32].

Binders can be classified into two different types: inorganic binders and organic binders [33]. Kaolin, bentonite, kaolinite, and montmorillonite are aluminosilicate clays that are traditionally used as a binder; however, they influence the properties of shaped zeolites [34]. The preference of organic binders is that, unlike inorganic binders, they decompose under oxidizing conditions and leave no residue so as to ensure that micropores are not blocked.

To optimize the properties of granules, different organic binders in several percentages were used; then, the mechanical and physical properties of products were studied. In this project, polyvinyl alcohol (PVA) and polyethylene glycol (PEG) were used as organic binders.

2. Materials and methods

2.1. Synthesis of zeolite 13X

Colloidal silica (Aldrich, 30 wt.% suspension in water), sodium aluminate (Merck), sodium hydroxide (Merck), and deionized water were used to get a hydrogel solution with the molar composition of $3.5Na_2O{:}Al_2O_3{:}2.9SiO_2{:}150H_2O$ [35] for the hydrothermal synthesis of zeolite 13X. The mixture was aged at room temperature for 40 minutes, while it was mixed with a magnetic stirrer and transferred into a Teflon lined hydrothermal synthesis autoclave reactor and was heated at 90°C for 48 hours. The product was filtered and washed with deionized water until the pH value reached about 9. It was dried at room temperature and, finally, milled in an agate mortar.

2.2. Granulation by using PVA

The aqueous solution containing 2, 4, 6, 8, and 10 wt.% of PVA (Merck, 72000 g/mol, hydrolyzed >98%) with respect to zeolite powder was made. After that, it was mixed with milled zeolite powder and the appropriate amount of deionized water to convert the mixture into the paste. Prepared pastes were shaped into the spherical granules with an average diameter of 3.2 mm by using a lab-sized disc-type granulator and were dried at room temperature for 24 hours. In order to remove water and prevent the appearance of cracks in the products, granules were dried in an electric oven at 70°C for 2 hours. Finally, samples were placed in a ceramic crucible and debinded and calcined in the muffle furnace at the thermal program, according to Figure 1.

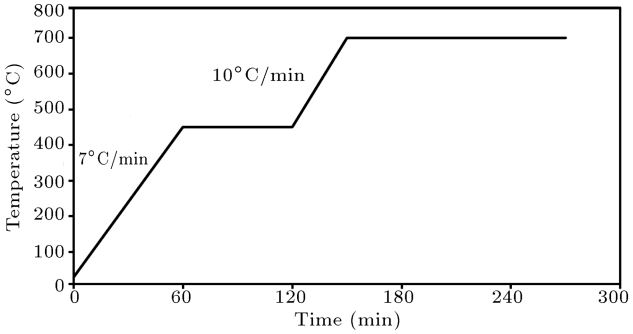

Figure 1. Thermal program of debinding and calcining.

2.3. Granulation by using PVA and PEG

The effect of adding PEG (Merck, 20000 g/mol) as a binder and plasticizer was studied. The aqueous solutions containing 0.25, 0.5, 1.5, and 3 wt.% of PEG with respect to zeolite powder were mixed with zeolite 13X powder, 6 wt.% PVA solution, required the amount of deionized water, and converted the mixture into pastes and, then, were shaped. Then, granules were dried at room temperature and, after that, were dried at 70°C for 2 hours again. Furnace temperature for debinding and calcination is as follows: from room temperature increased to 450°C at 7 °C/min and, then, held for 1 hours. Finally, the temperature increased to 700°C at 10°C min^{-1} and, then, was held at 290°C for 2 hours, as shown in Figure 1.

2.4. Characterization

The X-ray powder diffraction (XRD) patterns of synthesized zeolite 13X and granulated sample containing 6 wt.% PVA (after calcination at 700°C) were taken by STOE powder diffraction system using Cu-K_α radiation (40 kV, 40 mA) of wavelength 1.54060 Å with 0.06° step size and 1-second step time from 1 to 40°. The nitrogen adsorption-desorption isotherm, specific surface area, and pore size of the samples were measured with a micromeritics model ASAP2020 with surface area and porosity analyzer at 77 K after outgassing the samples at 300°C for 3 hours. The crush strength of samples was measured according to ASTM D 61 75-03. The morphology analysis of the samples was carried out by using a scanning electron microscopy (SEM) (KYKT-EM3200). Samples were gold coated prior to measurement. Thermal analysis of samples was carried out by a Bahr STA-503 instrument. Uncalcined samples were loaded in an alumina crucible and, then, heated to 1200°C with a heating rate of 10°C/min under air atmosphere with a flow rate of 50 mL/min.

2.5. CO_2 adsorption measurement

The volumetric method was used to investigate CO_2 adsorption capacity of samples by setup, as shown in Figure 2. Then, 1 g of the sample was loaded in the adsorption cell and was attached to the system. The existing gas inside the system was swept out with

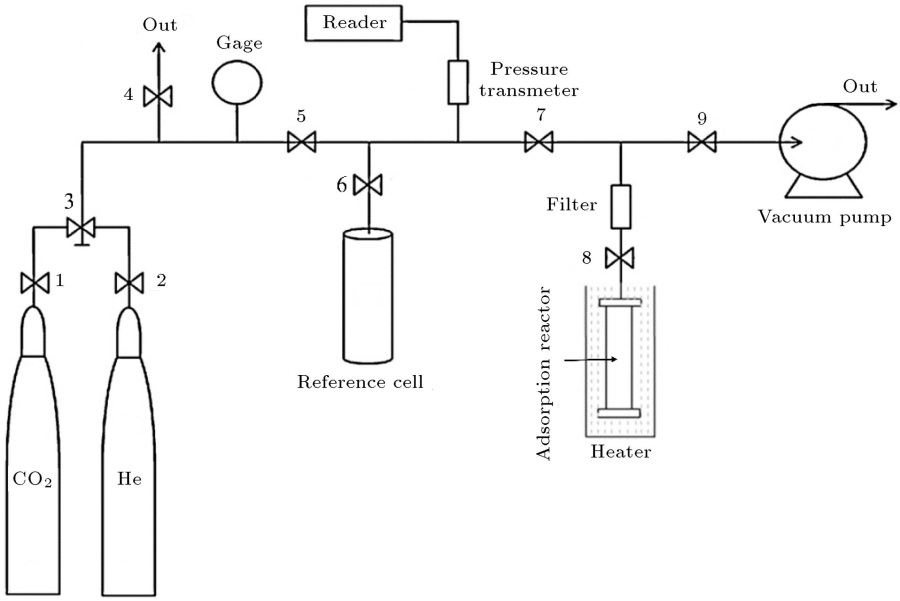

Figure 2. Setup for CO_2 adsorption measurement.

helium. For degassing the system, Valves 1, 2, and 4 were closed, and other valves were opened; then, the vacuum pump was turned on, and the system was vacuumed at a heating temperature of 250°C for 90 minutes. Afterward, Valves 5, 8, and 9 were closed, and the system was cooled to ambient temperature. To perform an adsorption test, the valve of ultra-high purity carbon dioxide cylinder (99.999%) and Valve 5 were opened to balance the desired pressure. Then, Valve 8 was immediately opened, and the pressure in adsorption cell decreased. The pressure of adsorption cell decreased due to the adsorption dead volume in the reactor. The dead volume was measured by the helium test and subtracted from the total pressure change. In addition, the decrease of exact pressure due to carbon dioxide adsorption was calculated.

3. Results and discussion

The X-ray diffraction patterns of synthesized zeolite 13X powder and prepared granules having 6% PVA after calcination at 700°C for two hours are shown in Figure 3. The XRD pattern of zeolite 13X powder matches that of the Na-X zeolite [36], representing the successful synthesis. The location of the reflection lines remains constant for the granulated sample, indicating that the structure of zeolite 13X was well preserved; however, the intensities slightly reduced due to the effect of calcination on crystallinity of samples.

Figure 4 shows the SEM images of zeolite 13X powder and granulated samples using 6 wt.% and 10 wt.% PVA after calcination. The crystals of zeolite 13X powder confirm their successful synthesis. It can be seen that well regular shape and morphology

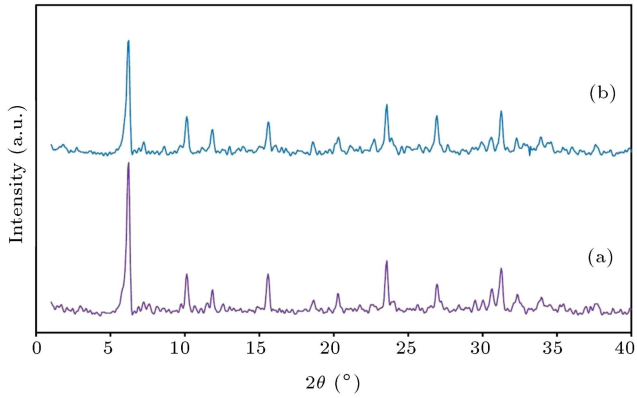

Figure 3. (a) XRD patterns of zeolite 13X powder. (b) Granule prepared using 6 wt.% PVA after calcination.

are in granulated samples. According to the SEM image of the granulated sample using 10 wt.% PVA (Figure 4(c)), PVA binder close to zeolite crystals, it is indicated that the binder removal is incomplete.

3.1. Granules prepared using PVA

Figure 5 shows the variation in average pore size with PVA content. According to the figure, the average pore size of samples increased by increasing PVA content. The application of more PVA amount in the paste results in the formation of larger pores after calcination and an increase in pore size. Average pore size of samples with 10 wt.% PVA increased by 9.41% compared with those prepared using 2 wt.% PVA binder (from 1.8561 nm for 2% to 2.0309 nm for 10 wt.%).

Based on Figure 6, for the samples prepared using different PVA percentages, as PVA increases, the specific surface area reaches a maximum amount

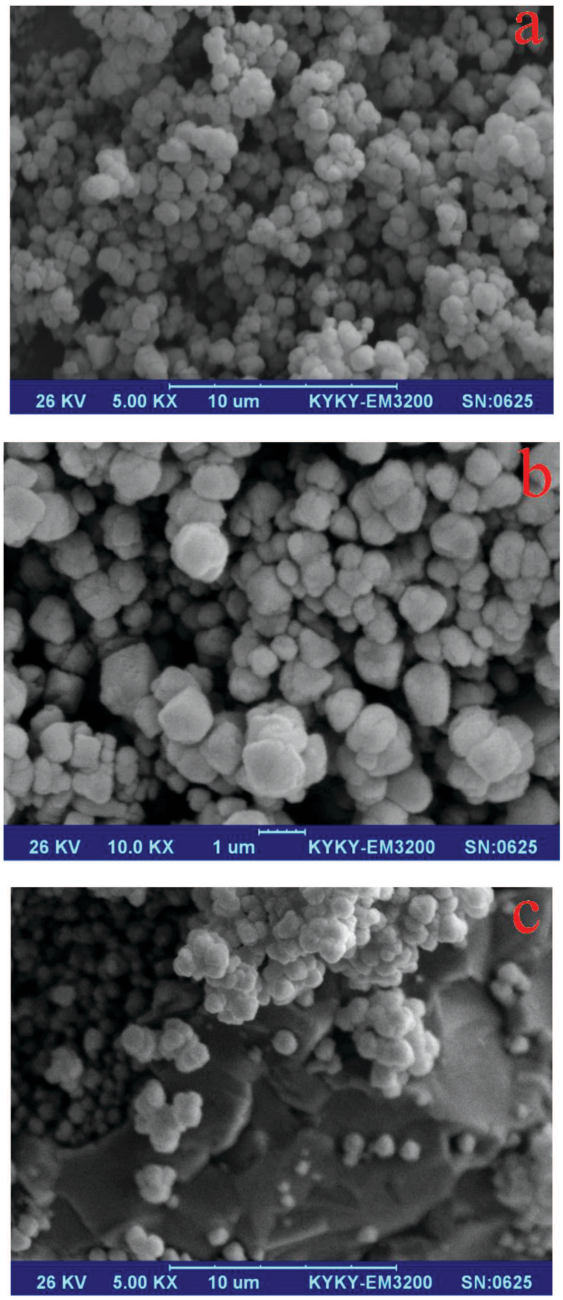

Figure 4. SEM image of zeolite 13X powder (a) granule prepared using 6 wt.% PVA (b) and 10 wt.% PVA (c) after calcination.

and, then, decreases. Granules with 2 wt.% PVA had the lowest specific surface area (507.8494 m^2/g). Increasing binder amount to 4 and 6 wt.% increases the specific surface area to 542.7279 and 612.9750 m^2/g, respectively. A further increase in PVA amount decreases the specific surface area to 575.0992 and 531.7569 m^2/g for 8 and 10 wt.%, respectively. An increase in the specific surface area from 2 to 6 wt.% PVA results from the vaporization of PVA and left pores after calcination. However, the decrease of the specific surface area for samples containing more than

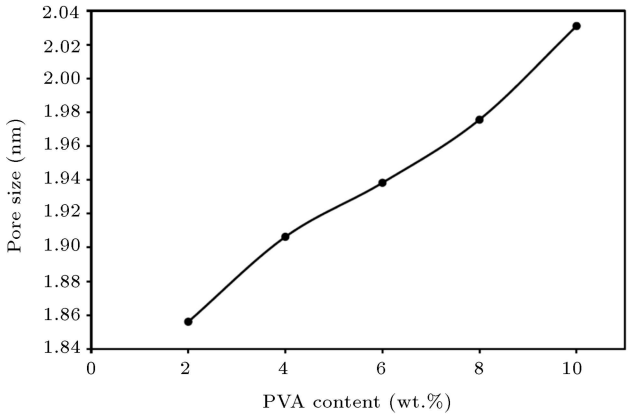

Figure 5. Effect of PVA amount on the average pore size of granules.

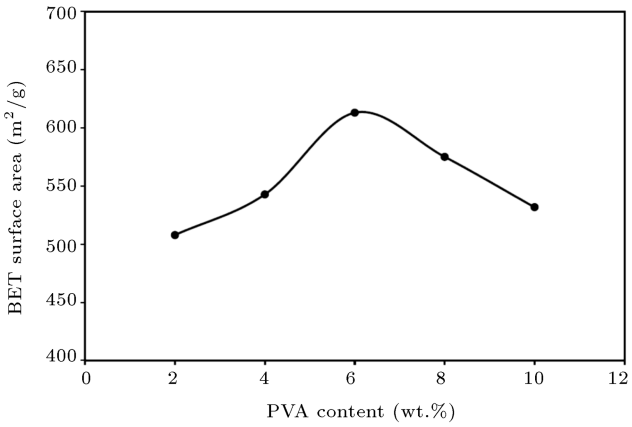

Figure 6. Effect of PVA amount on the specific surface area of granules.

6 wt.% amount of PVA can be related to incomplete burnout of PVA and its residual carbon. The presence of PVA binder in the granule prepared using 10 wt.% as a result of incomplete binder removal is obvious in Figure 4(c). Moreover, carbonaceous residue remained after burnout of high PVA content samples, causing no change in the total pore volume. However, due to an increase in average pore size, the specific surface area is decreased. Variations in the total pore volume and average pore size by increasing the PVA content in granules are listed in Table 1.

As can be seen in Figure 7, by increasing the PVA amount in the mixture, the crushing strength gradually decreases. It appears that the decrease of strength results from the difference in the porosity level of the samples. Pore size distribution curves of these samples are shown in Figure 8. The granules prepared using more PVA amounts have greater porosity after calcination, and the removal of binder and the existence of more cavities in these samples reduce the mechanical strength. The crushing strengths for samples with 2-10 wt.% PVA are 114.22, 63.02, 33.79, 23.03, and 19.40 N, respectively.

Table 1. Effect of PVA amount on the total pore volume and average pore diameter of granules.

PVA content	Total pore volume (cm^3/g)	Average pore diameter (nm)
2%	0.2911	1.8561
4%	0.2751	1.9063
6%	0.2689	1.9382
8%	0.2651	1.9756
10%	0.2640	2.0303

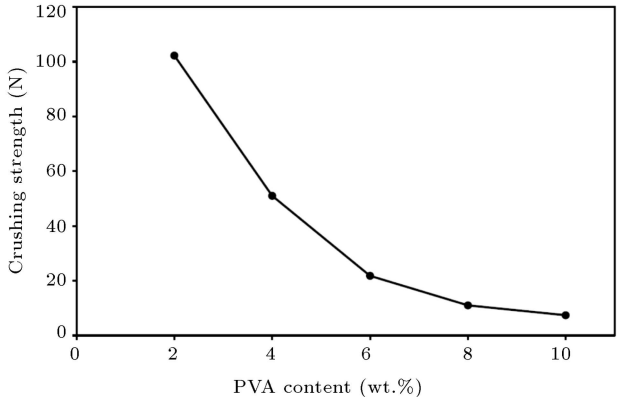

Figure 7. Effect of PVA amount on the crushing strength of granules.

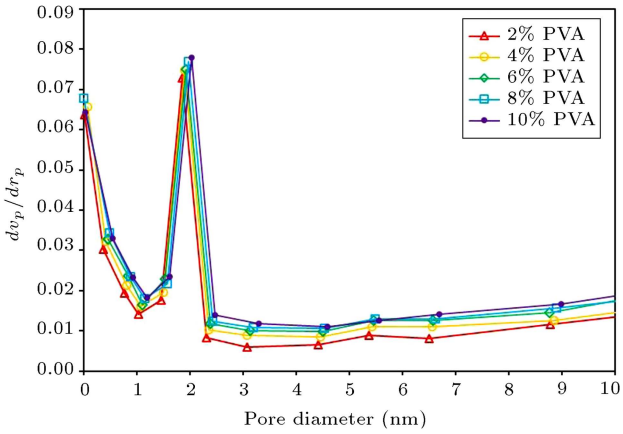

Figure 8. Pore size distribution of the samples prepared using different PVA percentages.

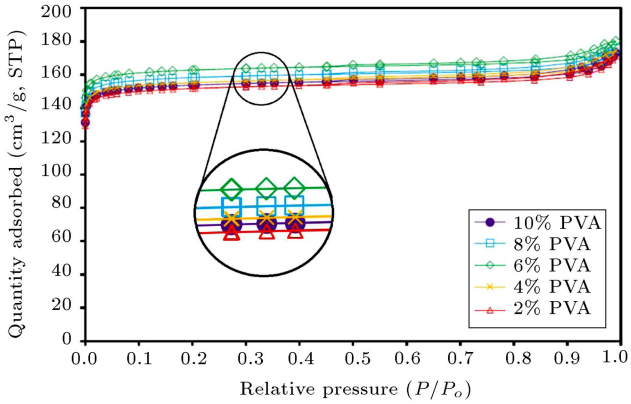

Figure 9. Effect of PVA amount on N_2 adsorption-desorption isotherm.

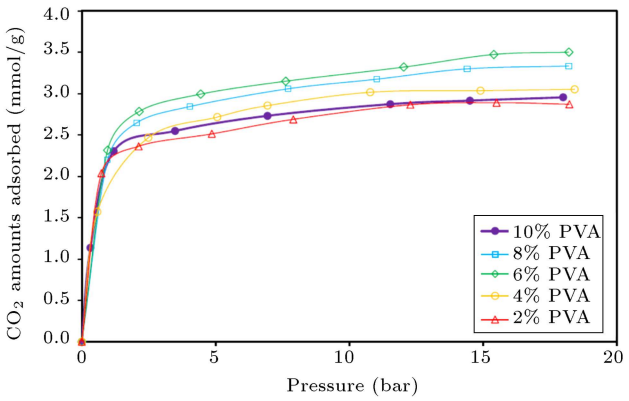

Figure 10. Effect of PVA amount on CO_2 adsorption capacity.

In order to investigate the effect of PVA amount on gas adsorption of produced granules, the results of N_2 adsorption-desorption isotherms and CO_2 adsorption capacities are illustrated in Figures 9 and 10, respectively. The N_2 adsorption isotherms of the granulated samples are typically of type I, which is a signature characteristic of microporous materials. As observed, N_2 adsorption capacity increases with PVA content up to 6 wt.% and, then, decreases by a greater increase in PVA content that can result from variations in the specific surface area. Moreover, CO_2 adsorption capacity shows the same trend. The higher values of the CO_2 adsorption capacity were obtained for the granules with the highest N_2 adsorption capacity and specific surface area (6 wt.% of PVA).

Moreover, the thermal properties of the granules containing 6 wt.% of PVA were investigated by TG/DTA analysis, and the results are shown in Figure 11. DTA plot of the sample at 10°C/min shows a broad endothermic peak between 50 and 200°C, which results from water present in cages and channels of the zeolite framework and water trapped within the binder. This exothermic peak is associated with the mass loss in this temperature range in TGA graph. A large, yet sharp, exothermic peak occurring from 250 to 500°C

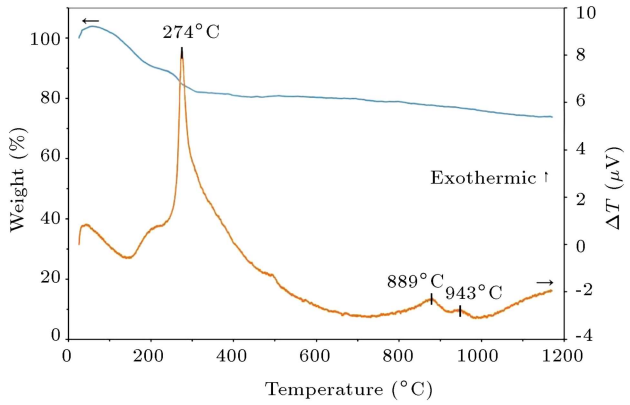

Figure 11. TGA and DTA profiles of the granules containing 6 wt.% of PVA.

and centering at 274°C is thought to be caused by PVA burnout. This phenomenon is shown with a small weight loss stage in TGA profile. At 889 and 943°C, there are two exothermic peaks in DTA curve that are not associated with any weight loss. Therefore, these peaks should correspond to the collapse of the zeolite framework in two stages.

3.2. Granules prepared using PVA and PEG

Figures 12 and 13 illustrate the effect of PEG amount on the average pore size and specific surface area, respectively. Both of the average pore size and specific surface area increased with the increase of plasticizer content. The values of average pore size and specific surface area for different percentages of PEG were found to be 1.9382, 1.9419, 1.9466, 1.9519, 1.9931 nm and 612.9750, 622.7558, 631.4400, 645.0985, 667.2166 m^2/g for 0, 0.25, 0.5, 1, and 3 wt.% amounts of PEG, respectively. This increase is attributed to PEG burnout after calcination.

The variation in the crushing strength with PEG amount in the mixture is presented in Figure 14. As can be seen, the crushing strength gradually decreases with an increase in PEG content. The effect of PEG in the reduction of the mechanical strength is the same as that of PVA; however, since PEG is added in less amounts, there is a minor reduction in the crushing strength. The crushing strengths for the samples with 0, 0.25, 0.5, 1, and 3 wt.% PEG are 33.79, 32.05, 29.91, 25.33, and 19.80 N, respectively.

The effect of PEG amount on the N_2 adsorption-desorption curves is illustrated in Figure 15. All samples exhibit very close isotherms, and all of them correspond to typical type I. N_2 adsorption capacity slightly increases by augmenting PEG, thus increasing the surface area.

Figure 16 shows the adsorption isotherms of CO_2 on the granules prepared with different PEG amounts. By increasing the PEG content, the value of the CO_2 adsorption capacity is partially increased. This

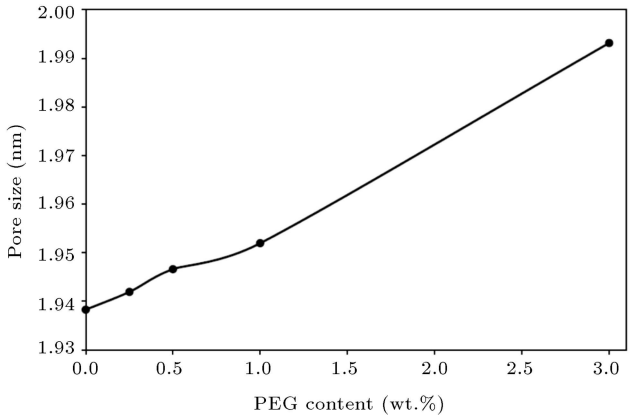

Figure 12. Effect of PEG amount on the average pore size of granules.

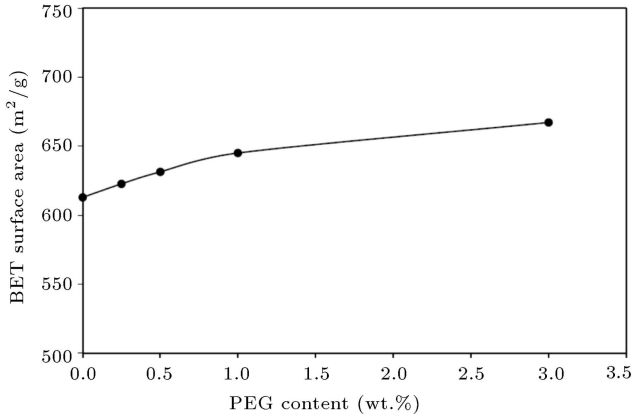

Figure 13. Effect of PEG amount on the specific surface area of granules.

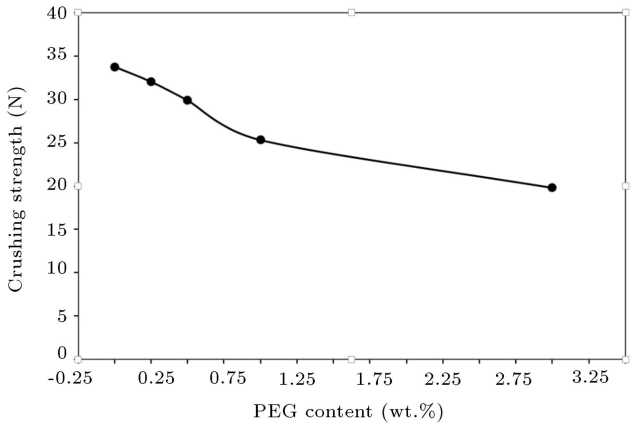

Figure 14. Effect of PEG amount on the crushing strength of granules.

increase is negligible for the samples containing 0.25, 0.5, and 1wt.% amounts of PEG.

4. Conclusion

Organic binders were used to shape the NaX zeolite powder into spherical granules. The binder content

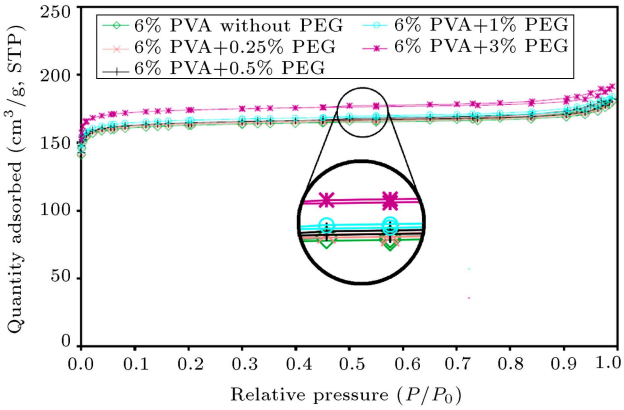

Figure 15. Effect of PEG amount on N_2 adsorption-desorption isotherm.

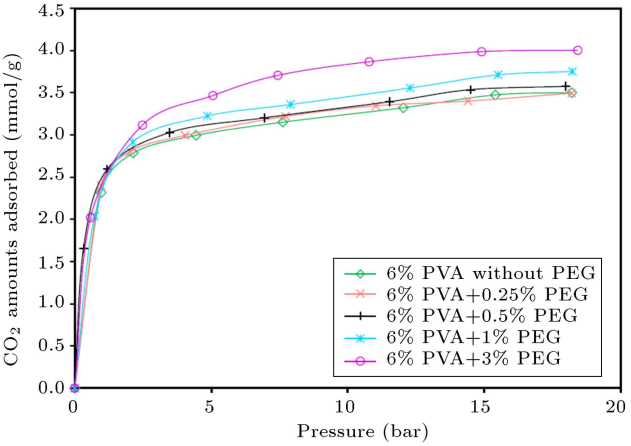

Figure 16. Effect of PEG amount on CO_2 adsorption capacity.

in the mixture strongly affects the properties of adsorbents. Since organic binders decompose in thermal processes, the appropriate amount of organic binders causes an increase in average pore size, surface area, and CO_2 adsorption capacity. Although incomplete debinding for further binder amounts was observed, the decrease of average pore size, surface area, and CO_2 adsorption capacity was detected, too. The application of large amounts of the binder was considered unfavorable from a mechanical strength viewpoint.

The best condition for the spherical adsorbents close to the mechanical and physical properties of products can be obtained when the amount of PVA is 6 wt.%. For the samples prepared using both PVA and PEG, the 0.25 wt.% amount showed the best properties.

References

1. Kadish, K., Guilard, R., and Smith, K.M., *The Porphyrin Handbook: Phthalocyanines: Properties and Materials*, Elsevier Science (2006).
2. Bhatia, S., *Zeolite Catalysts: Principles and Applications*, Taylor & Francis (1989).
3. Flanigen, E.M., Broach, R.W., and Wilson, S.T. "Introduction", In *Zeolites in Industrial Separation and Catalysis*, pp. 1-26, Wiley-VCH Verlag GmbH & Co. KGaA (2010).
4. Acton, Q.A., *Fluorine Compounds-Advances in Research and Application*, 2013 Edition", Scholarly Editions (2013).
5. Broach, R.W. "Zeolite types and structures" In *Zeolites in Industrial Separation and Catalysis*, pp. 27-59, Wiley-VCH Verlag GmbH & Co. KGaA (2010).
6. M'Sirdi, N., Namaane, A., Howlett, R.J., and Jain, L.C., *Proceedings of the 3rd International Conference on Sustainability in Energy and Buildings (SEB' 11)*, Springer (2012).
7. Khopkar, S.M., *Basic Concepts of Analytical Chemistry*, New Age International Publishers (1998).
8. Miao, T., Ju, S., and Xue, F. "Selectivity adsorption of thiophene alkylated derivatives over modified Cu^+-13X zeolite", *J. Rare Earth*, **30**(8), pp. 807-813 (2012).
9. Arslan, A. and Veli, S. "Zeolite 13X for adsorption of ammonium ions from aqueous solutions and hen slaughterhouse wastewaters", *J. Taiwan Inst. Chem. Eng.*, **43**(3), pp. 393-398 (2012).
10. Yu, X.H., Lü, H.L., Zhou, G.W., Zhou, L.G., and Zhang, Y.C. "Absorption of methyl orange by modified fly zeolites", *Adv. Mat. Res.*, **476-478**, pp. 1365-1369 (2012).
11. Jinka, K.M., Sebastian, J., and Jasra, R.V. "Epoxidation of cycloalkenes with cobalt(II)-exchanged zeolite X catalysts using molecular oxygen", *J. Mol. Catal. A: Chem.*, **274**(1-2), pp. 33-41 (2007).
12. Sievers, C., Liebert, J.S., Stratmann, M.M., Olindo, R., and Lercher, J.A. "Comparison of zeolites LaX and LaY as catalysts for isobutane/2-butene alkylation", *Appl. Catal. A, General*, **336**(1-2), pp. 89-100 (2008).
13. Soontornworajit, B., Wannatong, L., Hiamtup, P., Niamlang, S., Chotpattananont, D., Sirivat, A., and Schwank, J. "Induced interaction between polypyrrole and SO_2 via molecular sieve 13X", *Mater. Sci. Eng. B*, **136**(1), pp. 78-86 (2007).
14. Mohammadi, T. "Ion-exchanged zeolite X membranes: synthesis and characterisation", *Memb. Tech.*, **2008**(3), pp. 9-11 (2008).
15. Ursini, O., Lilla, E., and Montanari, R. "The investigation on cationic exchange capacity of zeolites: The use as selective ion trappers in the electrokinetic soil technique", *J. Hazard. Mater.*, **137**(2), pp. 1079-1088 (2006).
16. Purna Chandra Rao, G., Satyaveni, S., Ramesh, A., Seshaiah, K., Murthy, K.S.N., and Choudary, N.V. "Sorption of cadmium and zinc from aqueous solutions by zeolite 4A, zeolite 13X and bentonite", *J. Environ. Manage.*, **81**(3), pp. 265-272 (2006).
17. Yurekli, Y. "Removal of heavy metals in wastewater by using zeolite nano-particles impregnated polysulfone membranes", *J. Hazard. Mater.*, **309**, pp. 53-64 (2016).

18. Turnes Palomino, G., Otero Areán, C., and Llop Carayol, M.R. "Hydrogen adsorption on the faujasite-type zeolite Mg-X: An IR spectroscopic and thermodynamic study", *Appl. Surf. Sci.*, **256**(17), pp. 5281-5284 (2010).

19. Prasanth, K.P., Pillai, R.S., Bajaj, H.C., Jasra, R.V., Chung, H.D., Kim, T.H., and Song, S.D. "Adsorption of hydrogen in nickel and rhodium exchanged zeolite X". *Int. J. Hydrogen Energy*, **33**(2), pp. 735-745 (2008).

20. Silva, J.A.C., Schumann, K., and Rodrigues, A.E. "Sorption and kinetics of CO_2 and CH_4 in binderless beads of 13X zeolite", *Microporous Mesoporous Mater.*, **158**(0), pp. 219-228 (2012).

21. Jayaraman, A., Yang, R., Cho, S.H., Bhat, T.G., and Choudary, V. "Adsorption of nitrogen, oxygen and argon on Na-CeX zeolites", *Adsorption*, **8**(4), pp. 271-278 (2002).

22. Chen, C., Park, D.W., and Ahn, W.S. "CO_2 capture using zeolite 13X prepared from bentonite", *Appl. Surf. Sci.*, **292**(0), pp. 63-67 (2014).

23. Arefi Pour, A., Sharifnia, S., NeishaboriSalehi, R., and Ghodrati, M. "Performance evaluation of clinoptilolite and 13X zeolites in CO_2 separation from CO_2/CH_4 mixture", *J. Nat. Gas Sci. Eng.*, **26**, pp. 1246-1253 (2015).

24. Songolzadeh, M., Soleimani, M., and Takht Ravanchi, M. "Using modified Avrami kinetic and two component isotherm equation for modeling of CO_2/N_2 adsorption over a 13X zeolite bed", *J. Nat. Gas Sci. Eng.*, **27**, Part 2, pp. 831-841 (2015).

25. Pillai, R.S., Peter, S.A., and Jasra, R.V. "CO_2 and N_2 adsorption in alkali metal ion exchanged X-Faujasite: Grand canonical Monte Carlo simulation and equilibrium adsorption studies", *Microporous Mesoporous Mater.*, **162**, pp. 143-151 (2012).

26. Chen, C., Kim, S.S., Cho, W.S., and Ahn, W.S. "Polyethylenimine-incorporated zeolite 13X with mesoporosity for post-combustion CO_2 capture", *Appl. Surf. Sci.*, **332**, pp. 167-171 (2015).

27. Creamer, A.E. and Gao, B., *Carbon Dioxide Capture: An Effective Way to Combat Global Warming*, Springer International Publishing (2015).

28. Anbia, M. and Hoseini, V. "Enhancement of CO_2 adsorption on nanoporous chromium terephthalate (MIL-101) by amine modification", *J. Nat. Gas Chem.*, **21**(3), pp. 339-343 (2012).

29. Anbia, M., Hoseini, V., and Mandegarzad, S. "Synthesis and characterization of nanocomposite MCM-48-PEHA-DEA and its application as CO_2 adsorbent", *Korean J. Chem. Eng.*, **29**(12), pp. 1776-1781 (2012).

30. Salehi, S., Anbia, M., Hosseiny, A.H., and Sepehrian, M. "Enhancement of CO_2 adsorption on polyethylenimine functionalized multiwalled carbon nanotubes/Cd-nanozeolite composites", *J. Mol. Struct.*, **1173**, pp. 792-800 (2018).

31. Bezerra, D.P., Silva, F.W.M.d., Moura, P.A.S.d., Sousa, A.G.S., Vieira, R.S., Rodriguez-Castellon, E., and Azevedo, D.C.S. "CO_2 adsorption in amine-grafted zeolite 13X", *Appl. Surf. Sci.*, **314**(0), pp. 314-321 (2014).

32. Sterte, J., Hedlund, J., and Tosheva, L. "Advanced materials and applications", In *Impact of Zeolites and other Porous Materials on the New Technologies at the Beginning of the New Millennium*, pp. 1437-1570, Elsevier Science (2002).

33. Gardziella, A., Pilato, L.A., and Knop, A., *Phenolic Resins: Chemistry, Applications, Standardization, Safety and Ecology*, Springer (2000).

34. Sulaymon, A.H. and Mahdi, A.S. "Spherical zeolite-binder agglomerates", *Chem. Eng. Res. Des.*, **77**(4), pp. 342-350 (1999).

35. Zhang, X., Tang, D., Zhang, M., and Yang, R. "Synthesis of NaX zeolite: Influence of crystallization time, temperature and batch molar ratio SiO_2/Al_2O_3 on the particulate properties of zeolite crystals", *Powder Technol.*, **235**(0), pp. 322-328 (2013).

36. Treacy, J. and Higgins, J.B., *Collection of Simulated XRD Powder Patterns for Zeolites*, Elsevier Science (2001).

Biographies

Mansoor Anbia obtained his MS (1993) and PhD degrees (2007) from Tehran Tarbiat Moallem University, Iran. His PhD program was under the supervision of Professor Vaghef Hossein. Dr. Anbia has been honored with several national and international scientific awards. He is currently a Full Professor at Iran University of Science and Technology. His research interests include inorganic ion-exchangers, mesoporous adsorbents, nanostructured new materials, chromatography (HTPLC, HPLC & GSC), removal of organic and inorganic pollutants from industrial effluents, purification methods for recovery of different chemical compounds from industrial waste, and application of new materials for use in different industrial plants.

Mahsa Aghaei received her BS degree in Pure Chemistry from Guilan University, Iran in 2011 and her MS degree in Analytical Chemistry from Iran University of Science and Technology, Tehran, Iran, 2014. She is a currently instrumental analysis and general laboratory technician at Tehran University of Medical Sciences Core Facility (TCF).